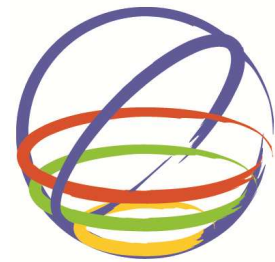


Efficiency of Different Techniques in Seismic Strengthening of RC Beam-Column Joints

M. Coelho, P. Fernandes, J. Sena-Cruz & J. Barros

Universidade do Minho, Guimarães



15 WCEE
LISBOA 2012

SUMMARY:

In the last years several techniques have been proposed and used for the seismic strengthening of reinforced concrete (RC) beam-column joints using fiber reinforced polymers (FRP). The Near Surface Mounted (NSM) technique uses FRP bars or laminates inserted into grooves opened on the concrete cover and filled with epoxy adhesive. In the Mechanically Fastened and Externally Bonded Reinforcement (MF-EBR) technique, multidirectional laminates of carbon fiber reinforced polymers (MDL-CFRP) are simultaneously bonded with epoxy adhesive and mechanically fixed with anchors to the faces of the elements to be strengthened. With the aim of comparing the seismic efficiency of NSM and MF-EBR techniques, tests with RC joints, representative of the buildings construction practice in Southern European countries until the early 1970s were carried. The experimental campaign comprises cyclic tests on seven full-scale RC joints with distinct configurations when both, NSM and MF-EBR techniques, are used. The tests are described and the main results are presented and analyzed.

Keywords: RC Beam-Column Joint, CFRP, NSM and MF-EBR Strengthening Techniques

1. INTRODUCTION

The consequences of an earthquake in terms of damages, human losses and socio-economic impact, are quit known. When this natural phenomenon occurs the vulnerability of the existing reinforced concrete (RC) structures is sometimes revealed. In Portugal, until the eighties, the construction of RC buildings had significant deficiencies in the joint regions due to the lack of recommendations in terms of seismic action. In order to guarantee the safety of those buildings, their performance must be assured. Two distinct ways can be adopted in those cases where safety usage of the buildings is not verified: rebuilding or retrofitting. The latter is the more desired measure since it leads to less economical and ecological impacts.

In the last years several repairing and strengthening techniques have been proposed for upgrading RC beam-column joints. Those can be grouped as follows (Engindeniz et al. 2004): (i) repair with epoxy (injection of epoxy resin in the cracks of the elements lightly degraded); (ii) removal and replacement of concrete in the damaged areas; (iii) jacketing with RC layers, masonry blocks or steel plates; (iv) use of composite materials.

The present work intends to contribute to the knowledge in the use of composites materials for strengthening RC beam-column joints. Three different techniques of applying composites materials are used. The first, designated by Near-Surface Mounted (NSM), consists on the insertion of laminates (or rods) into slits opened on the concrete cover (Sena-Cruz, 2004). The second, designated Mechanically Fastened Reinforcement FRP (MF-FRP), consists on applying multi-directional laminates of glass and carbon fibres anchored to concrete elements (Bank, 2004). The last one, designated Mechanically Fastened and Externally Bonded Reinforcement (MF-EBR), consists on applying multi-directional laminates of carbon fibres (MDL-CFRP) simultaneously glued and anchored to concrete (Sena-Cruz et al., 2010)

To assess the potentialities of the efficiency of these three techniques in the seismic strengthening,

seven full-scale exterior RC beam-column joints were strengthened with distinct configurations and tested under cyclic loading. These joints were built in order to be representative of exterior beam-column connections of the buildings construction practice in Southern European countries until the early 1970s. In this paper the referred tests are described, and the obtained results are presented and discussed.

2. EXPERIMENTAL PROGRAM

2.1 Specimens and test setup

Figure 2.1 presents the geometry of the RC joints, as well as the detailing of the beam and column cross sections adopted for all specimens. In the beams, with a cross section of 300 mm wide and 400 mm height, the longitudinal reinforcement was composed of 4 steel bars of 12 mm diameter ($4\phi 12$) at both sides. The transverse reinforcement consists of 8 mm diameter stirrups spaced 200 mm. In the columns, with square cross-section of 300 mm edge, the longitudinal reinforcement was composed by $4\phi 12$ and the transverse reinforcement was formed by 8 mm diameter stirrups spaced 250 mm. The concrete cover was 20 mm thick for all the elements.

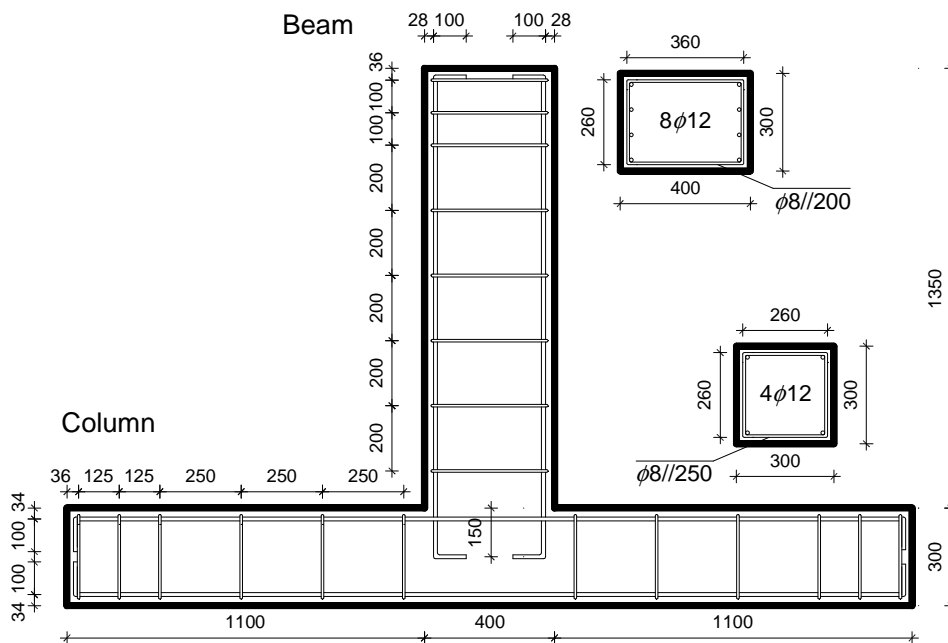


Figure 2.1. Beam-column joint specimen's geometry and reinforcement detailing. Note: all units in millimeters

Figure 2.2 shows the adopted test setup. The columns are simply supported at their extremities. The axial load at the ends of the columns was applied by hydraulic actuator (C3 in Figure 2.2.) to which was added one load cell (C4 in Figure 2.2). The transverse load at the top of the beam was applied by the hydraulic actuator servo-controlled C2 equipped with load cell C1 (see Figure 2.2) to measure the corresponding force. Figure 2.3 presents the location of the strain gauges (SG1-SG2) and linear variable differential transducers were used to register the strains in steel rebars and measure the displacements (LVDT1-LVDT8) along the specimen, respectively. Further details about the test configuration and instrumentation can be found elsewhere (Coelho, 2011).

All the tests were carried out under displacement control at C1 (see Figure 2.2). The imposed law consisted on applying complete reversal cycles throughout eighteen displacement levels of increasing amplitude: ± 1 mm, ± 2 mm, ± 4 mm, ± 6 mm, ± 10 mm, ± 15 mm, ± 20 mm, ± 25 mm, ± 30 mm, ± 40 mm, ± 50 mm, ± 60 mm. From level ± 1 mm to ± 4 mm only one complete cycle per displacement level was performed. From level ± 6 mm to the end of the test three complete cycles per level were applied. The maximum displacement defined was considered after preliminary test in the reference specimen.

To appraise the efficiency of different (MF-EBR, MF-FRP and NSM) in seismic strengthening of RC beam-column joints, an experimental program composed by seven joints was carried out (see Table 2.1). In this study six joints were strengthened with CFRP laminates according to the strengthening configurations and detailing represented in Figure 2.4. There were two major solutions, one that was designated “indirect” strengthening, because the strips were only placed on the front and rear faces of the joint and the laminate was not working on its appropriate direction (see Figure 2.4a), and one that was designated “direct” strengthening, because it had laminate strips on the lateral faces of the joint, which is a much proper direction for the laminate to work (see Figure 2.4b). Reference specimen was tested to compare and evaluate the performance of each technique.

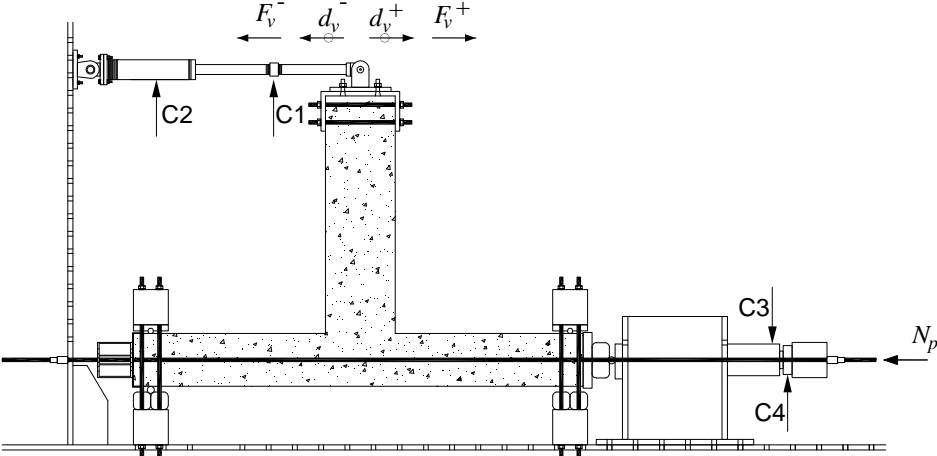


Figure 2.2. Test setup

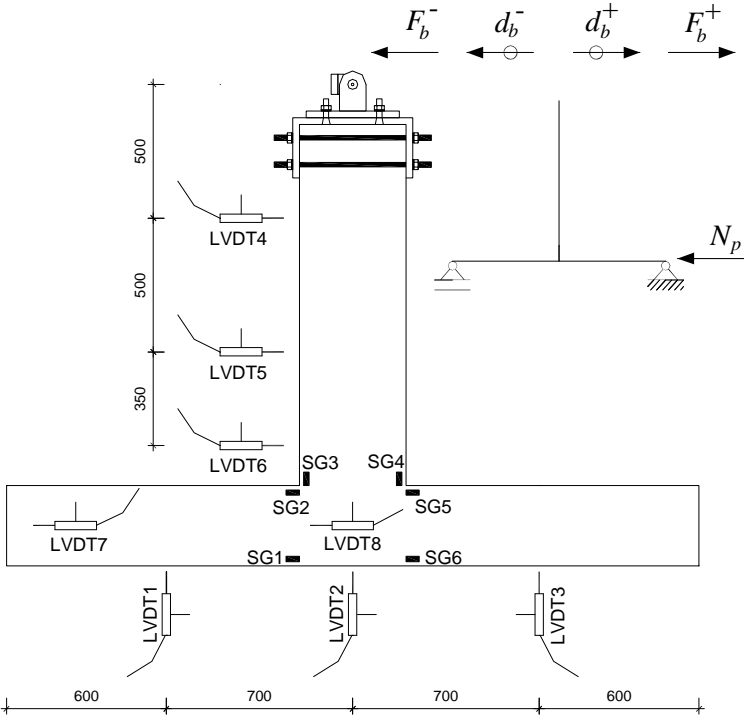


Figure 2.3. Instrumentation. Note: all units in millimeters

Before starting the cyclic test, an axial force of 220 kN was applied at the ends of the columns (by actuator C3). This axial force corresponds to a reduced axial force (v) of about 10%, which is a typical value for RC columns in external frames with spans of about 4 m, of buildings with 2 or 3 storeys. The axial force was kept constant during the entire cyclic test for all tested specimens.

Table 2.1. Experimental program

Specimen	Technique	N° of specimens	Laminate	t_f [mm]	w_f [mm]
REF	-	1	-	-	-
NSMi	NSM	1	UD-CFRP	1.4	10
NSMd	NSM	1			
MF-EBRi	MF-EBR	1	MDL-CFRP	2.1	30
MF-EBRib	MF-EBR	1			
MF-EBRd	MF-EBR	1			
MF-FRPd	MF-FRP	1			

2.2 Material characterization

Prior to the cyclic tests, mechanical material characterization of concrete, CFRP laminates and epoxy adhesive was performed.

The mechanical characterization of the concrete was assessed in two different dates by means of compression tests. For that purpose three cylindrical concrete specimens with a diameter of 150 mm and a height of 300 mm were tested for a concrete age of 28 days to evaluate the compressive strength according to the NP EN 12390-3:2009. The results indicated an average compressive strength of 24.6 MPa, with a coefficient of variation (CoV) of 1.86%. At the time of the joints tests five cylindrical concrete specimens were tested to evaluate the compressive strength and the modulus of elasticity according to the recommendation LNEC E397-1993. From the compression tests, an average compressive strength value of 32.08 MPa (CoV = 1.75%) and an average value of 26.98 GPa (CoV = 7.08%) for the modulus of elasticity, were obtained. The age of the concrete joints at the date of experimental program was about three months.

The steel of the longitudinal bars and stirrups was a typical A400 NR used in construction (NP EN 1992-1-1:2010). The main mechanical properties of the steel rebars were evaluated throughout tensile tests according to the EN 10 002-1:1990 (CEN, 1990). From these tests, for the longitudinal steel rebars of 12 mm diameter, average values of 465 MPa, 613 MPa and 194 GPa were obtained for the yielding and ultimate strengths, and for the modulus of elasticity, respectively. For the transverse steel rebars of 8 mm diameter, average values of 442 MPa, 569 MPa and 210 GPa were obtained for the yielding and ultimate strengths, and for the modulus of elasticity, respectively.

The MDL-CFRP used to strengthen the joints was designed and produced in the scope of the current research project. All the information related to its development and characterization is available elsewhere (Sena-Cruz et al., 2010). From this characterization, the following average values were obtained: tensile strength of 1866 MPa; modulus of elasticity of 118 MPa; strain at failure of 1.58%; bearing unclamped resistance of 316 MPa; bearing clamped resistance of 604 MPa; thickness of 2.07 mm.

The UD-CFRP laminate used in the present work, with a cross section of 1.4 mm thick and 10 mm wide, and a trademark CFK 150/2000, was provided in rolls of 100 m each, and was supplied by S&P® Clever Reinforcement Company. This laminate was composed of unidirectional carbon fibres agglutinated by an epoxy adhesive, and has a smooth external surface. Tensile properties of the CFRP were assessed by performing tensile tests according to ISO 527-5 (1997), adopting a displacement rate of 2 mm/min. To evaluate the modulus of elasticity, a clip gauge was mounted at middle region of each specimen. From the mechanical characterization, a modulus of elasticity, a tensile strength and a strain at peak stress of, respectively, 158 GPa (0.9%), 2435 MPa (CoV=5.8%) and 1.50% (CoV=4.7%) were obtained.

The S&P Resin 220 epoxy adhesive® was used to glue the MDL-CFRP and UD-CFRP to concrete surfaces. To mechanically fix the MDL-CFRP to concrete, a Hilti system composed by the resin HIT-HY 150 MAX, the HIT-V M8 8.8 threaded anchors and DIN 9021 washers was adopted. The anchors were pre-stressed using a torque of 40 N·m. The main properties of these materials can be found elsewhere (Sena-Cruz et al., 2010).

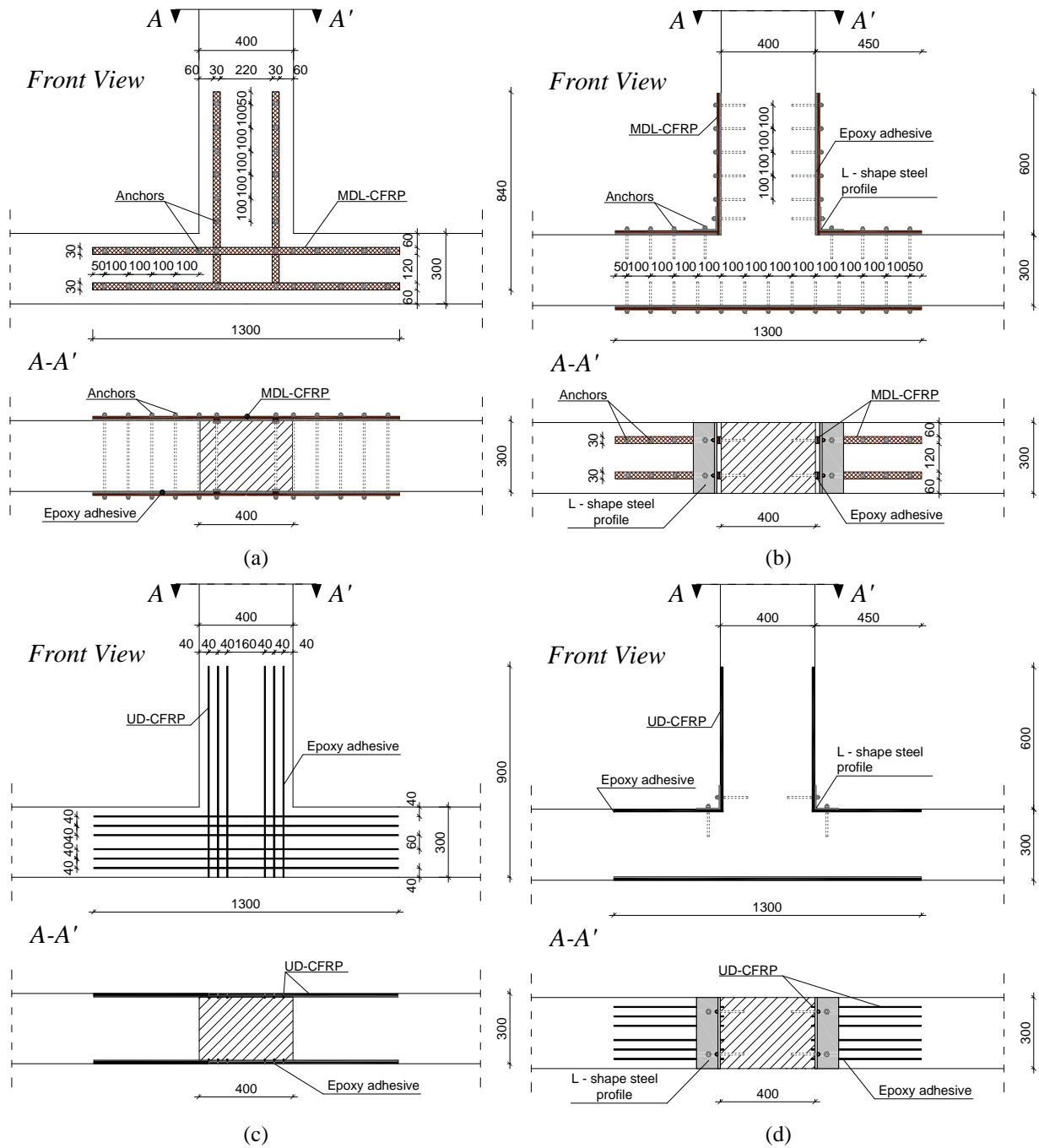


Figure 2.4. Strengthening solutions detailing: (a) MF-EBRi; (b) MF-EBRd; (c) NSMi; (d) NSMd

2.3 Preparation of the specimens

The preparation of the strengthened specimens required several steps. Figures 2.5 and 2.6 show the major steps of the strengthening procedures for the MF-EBR and MF-FRP techniques, respectively. Figure 2.7 presents the main steps for the NSM technique. All the details about these procedures can be found elsewhere (Coelho et al., 2011).

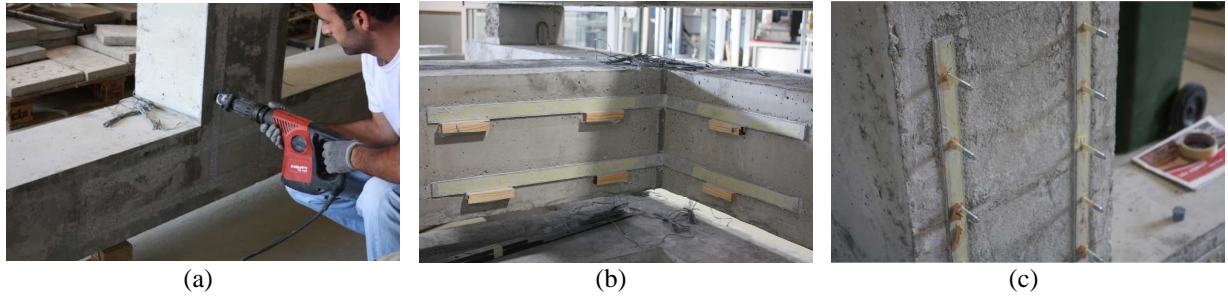


Figure 2.5. Strengthening procedure for the MF-EBR technique: (a) preparation of the concrete surface; (b) MDL-CFRP was placed on the concrete surface by pressing it against to concrete in order to create an uniform thickness of 1 to 2 mm of adhesive layer; (c) application of the anchors

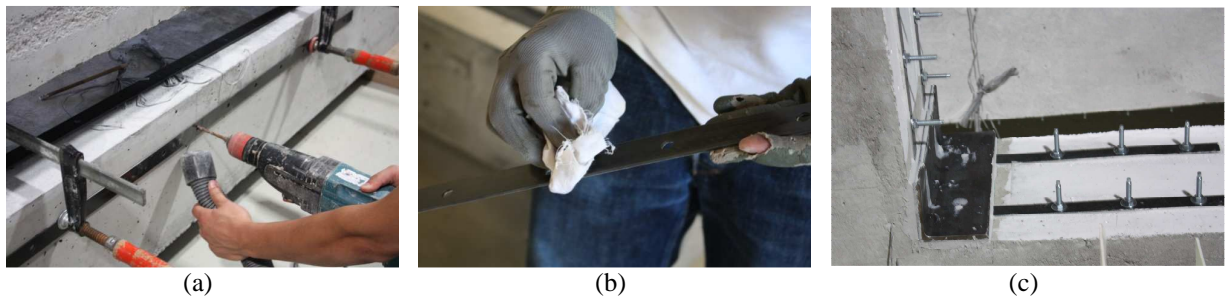


Figure 2.6. Strengthening procedure for the MF-FRP technique: (a) drilling holes with 10 mm diameter and 100 mm deep; (b) cleaning the MDL-CFRP with acetone; (c) specimen after strengthening

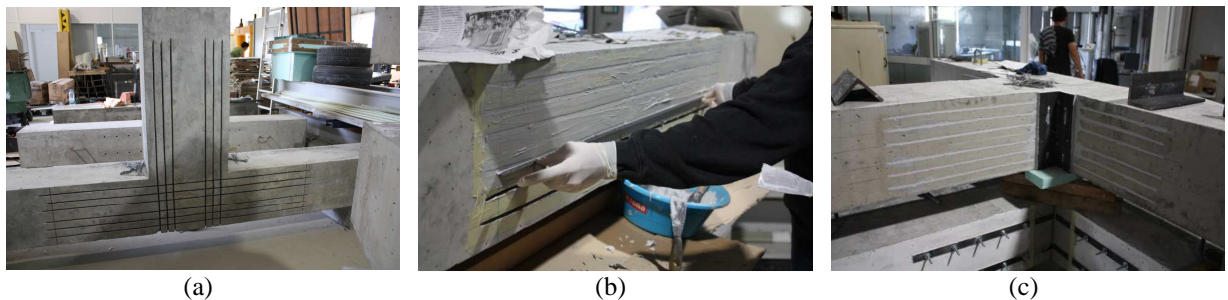


Figure 2.7. Strengthening procedure for the NSM technique: (a) cutting and cleaning the grooves; (b) UD-CFRP application; (c) L-shaped steel profile application

3. RESULTS

Table 3.1 resumes the main results obtained in the performed tests, while Figs. 3.1 and 3.2 depict the global response in terms of lateral force, F_b , versus lateral displacement, d_b , at the top of the beam, the corresponding envelopes and elasto-plastic approximation according to the EC8 (CEN, 2004). In this table $F_{b,cr}$ and $F_{b,max}$ are the loads at concrete crack initiation and maximum point, respectively, and $\delta_{b,cr}$ and $\delta_{b,max}$ are the corresponding vertical displacements at the top of the beam.

All the strengthened specimens presented an increment in the load carrying capacity when compared to the reference one. For the specimens strengthened with the MF-EBR technique the direct solution was the most efficient achieving an increment of load carrying capacity of 40% (MF-EBRd). The specimen strengthened with the MF-FRPd technique achieved an increment of 52% which was a surprise since it was expected that its result was lower or at most equal to the MF-EBRd. In fact, MF-FRPd only had fasteners while MF-EBRd had an epoxy adhesive in conjunction to the fasteners. The only plausible explanation for that can be related to a deficient application of the steel corners in this last one.

The specimens strengthened with the NSM technique presented both high level of performance. Increments of 75% and 52% where achieved for NSMi and NSMd, respectively. In the first one, the

maximum load was attained to a displacement of 39.97 mm, which proves the high performance of this technique.

Table 3.1. Main results obtained

Specimen	Negative Direction (d_b^-)						Positive Direction (d_b^+)						Failure Mode
	$\delta_{b,cr}$ [mm]	$F_{b,cr}$ [kN]	Cycle	$\delta_{b,max}$ [mm]	$F_{b,max}$ [kN]	Cycle	$\delta_{b,cr}$ [mm]	$F_{b,cr}$ [kN]	Cycle	$\delta_{b,max}$ [mm]	$F_{b,max}$ [kN]	Cycle	
REF	-1.01	-6.69	1	-8.92	-33.34	10	1.03	12.94	1	7.80	36.59	10	CR+SP
MF-EBRi	-2.04	-16.36	2	-13.59	-38.70 (16%)	15	1.99	21.95	2	9.99	39.58 (8%)	10	CR+SP+ DB+BF
MF-EBRib	-2.00	-16.69	2	-14.26	-40.24 (21%)	15	2.00	21.82	2	19.97	43.03 (18%)	20	CR+SP+ DB+BF
MF-EBRd	-1.99	-17.40	2	-9.15	-46.82 (40%)	10	2.02	26.07	2	8.17	49.07 (34%)	10	CR+SP+ DB+BF
MF-FRPd	-2.00	-18.86	2	-9.15	-46.36 (39%)	10	2.02	25.61	2	9.95	55.44 (52%)	10	CR+SP+ BF
NSMd	-2.02	-20.17	2	-10.01	-50.57 (52%)	15	1.98	21.99	2	9.02	51.88 (42%)	10	CR+SP
NSMi	-2.04	-15.42	2	-39.97	-58.26 (75%)	40	2.01	23.93	2	29.99	60.41 (65%)	30	CR+SP

Notes: values in brackets represent the increase from REF to strengthened specimens. Failure modes: CR – Cracking; SP – Concrete spalling at the corners; DB – Adhesive/concrete debonding; BF – MDL-CFRP bearing.

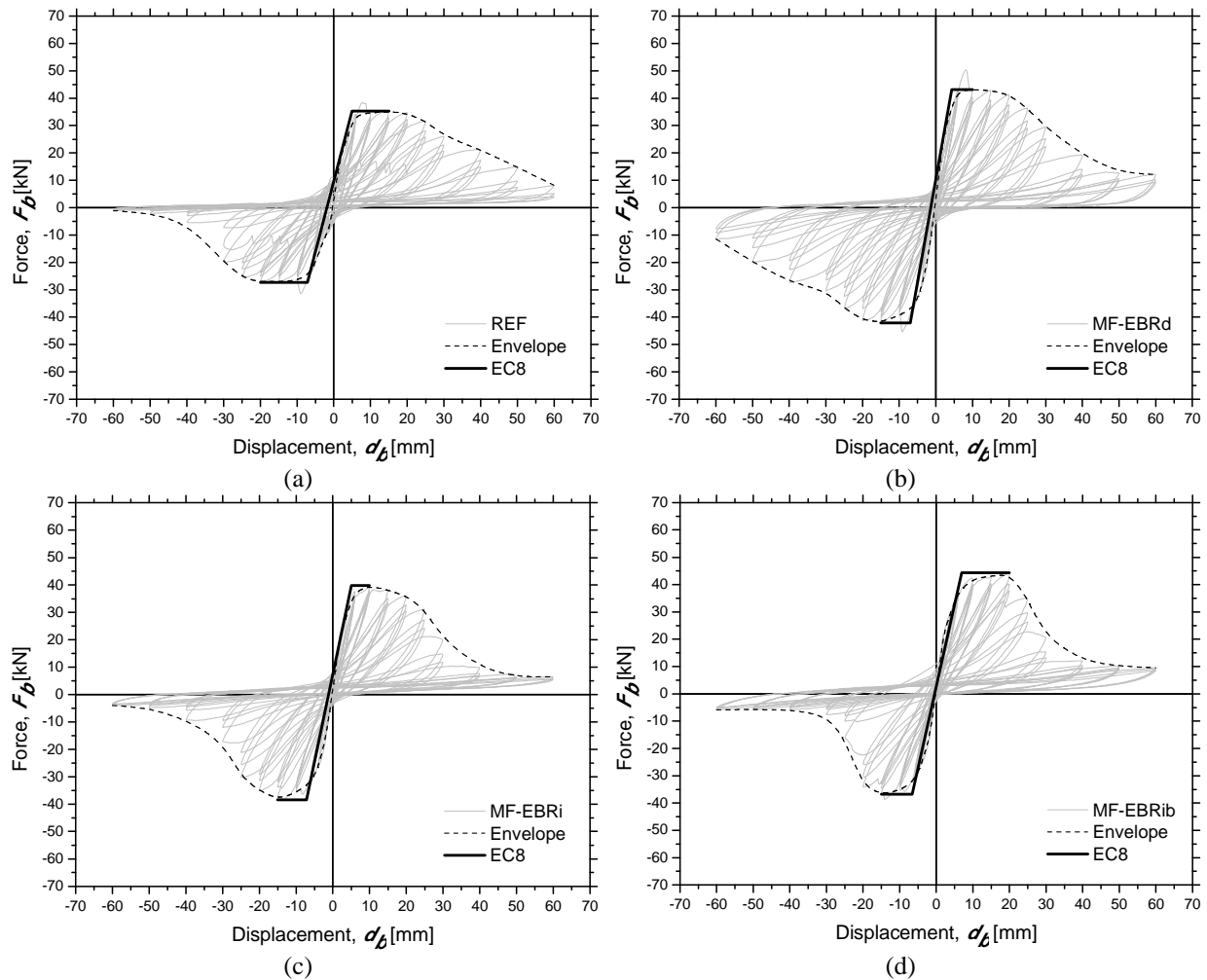


Figure 3.1. Force vs. displacement relationship: (a) REF; (b) MF-EBRd (c) MF-EBRi; (d) MF-EBRib

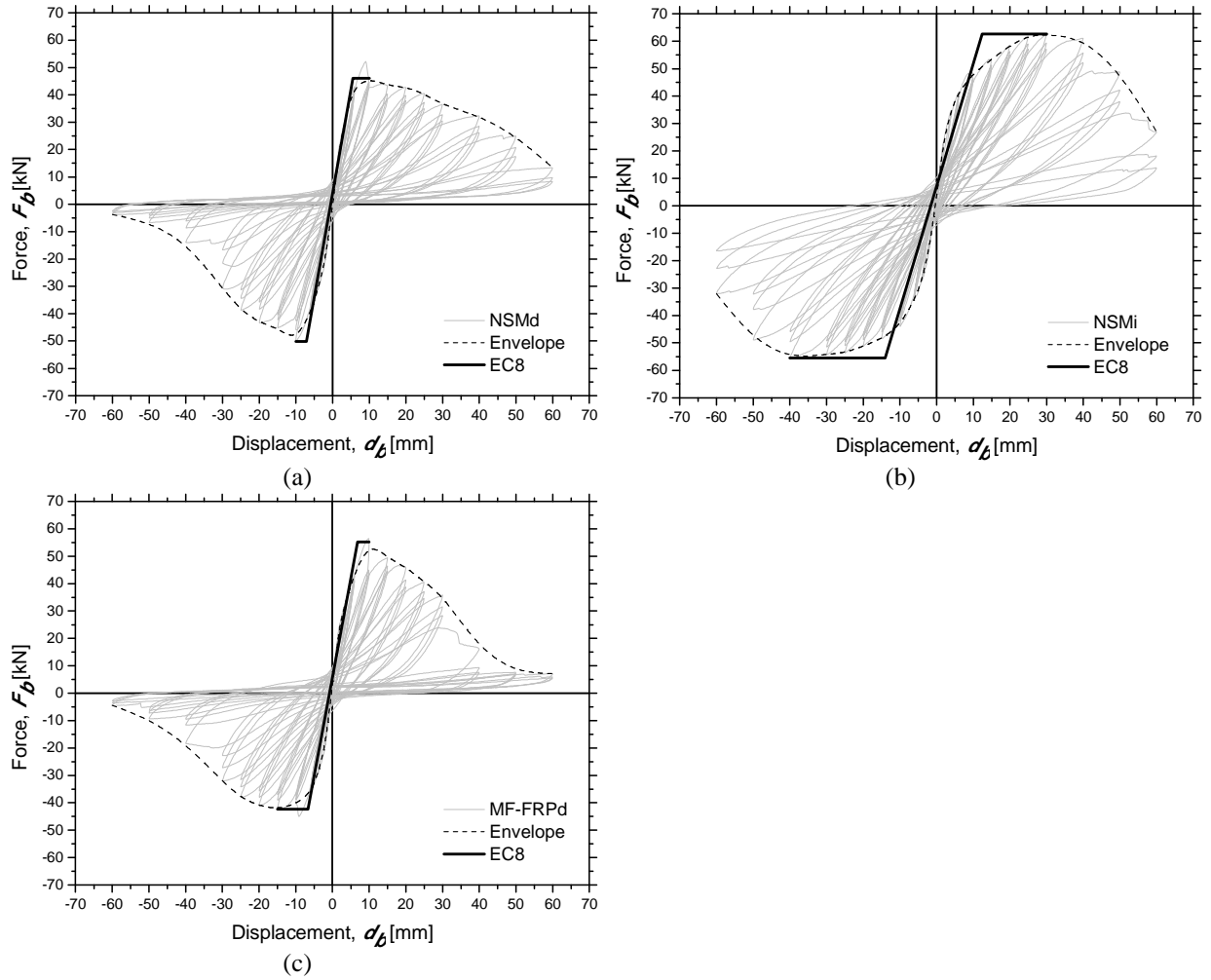


Figure 3.2. Force vs. displacement relationship: (a) NSMd; (b) NSMi; (c) MF-FRPd

In terms of initial stiffness, all the strengthened specimens present similar behaviour, being its degradation lower than the one revealed by the reference specimen.

Table 3.1 also contains the failure modes observed in the tested specimens which can be seen in Figure 3.3. Those were mainly composed by concrete cracking and spalling in the corners of the joints vicinity for all the specimens, debonding in the interface adhesive/concrete for the MF-EBR specimens and MDL-CFRP bearing failure for MF-EBR and MFR-FRP specimens.

As expected, the most affected area was the top face of the column near the middle of the joint. Another interesting remark was that for the specimens with indirect strengthening solutions, the damage began later than in the specimens with direct strengthening. But, if compared in terms of ultimate resistance, the direct solutions behaved better. That can be associated to a more proper location of the laminates and to the steel corners in the specimens with direct solutions. In fact, the steel corners delayed the concrete spalling in the corners of the joints.

For the NSM specimens, UD-CFRP rupture was observed in the NSMd while concrete cover delamination, including the UD-CFRP, was observed for the NSMi specimen.

Figure 3.4. presents a graphical view for the determination of the elasto-perfectly plastic force-displacement curve idealization from Annex B of the EN 1998-1:2004. Point A coincides with the maximum force reached during the tests in each direction, being (d_m^*, F_y^*) its coordinates. The parameter E_m^* is the deformation energy up to point A. The unknown point is the yield displacement of the idealized curve (d_y^*, F_y^*) . This point can be calculated by the following Eqn. 3.1.

$$d_y^* = 2 \left(d_m^* - \frac{E_m^*}{F_y^*} \right) \quad (3.1)$$

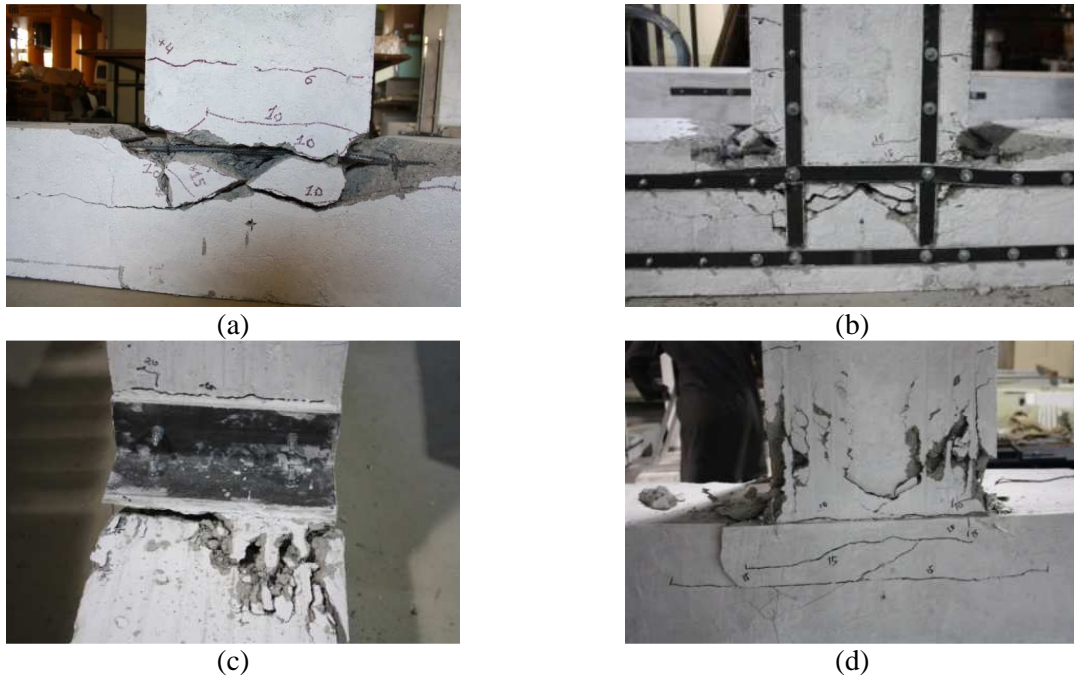


Figure 3.3. Failure modes: (a) buckling in the longitudinal steel; (b) MF-EBRi; (c) NSMd; (d) NSMi

Table 3.2 presents the values that were used to define the displacement ductility. In this table, d_y^- and d_y^+ are the yielding displacement in the idealized elasto-perfectly plastic curve in negative and positive directions, respectively; d_u^- and d_u^+ represent the ultimate displacements, for the same curves, in negative and positive directions, respectively. Assuming the displacement ductility ratio, μ , defined by Eqn. 3.2, Table 3.2 gives a comparison between all tested specimens for that ratio. According to the obtained results, it can be said that all the strengthened specimens yielded to less displacement ductility than the reference one. This behaviour is typical in the specimens strengthened with FRP's, in which the strength and stiffness increase and the ductility decrease.

$$\mu = \frac{d_u^- + d_u^+}{d_y^- + d_y^+} \quad (3.2)$$

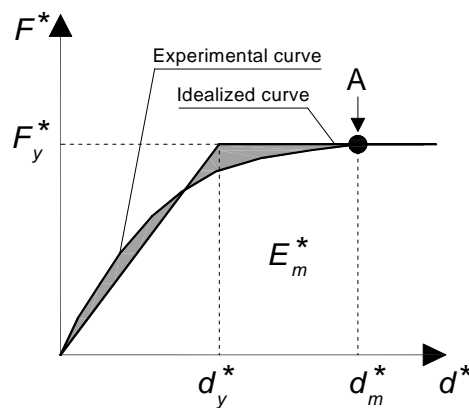


Figure 3.4. Idealized elasto perfectly plastic force vs. displacement relationship

In terms of dissipated energy, while in NSM specimens the direct one presented lower dissipated energy than the indirect specimen, in the MF specimens the opposite occurred. When comparing MF-EBRd and MF-FRPd, the expected higher level of energy dissipation in the first one was verified, mainly because of the presence of epoxy adhesive.

Table 3.2. Displacement ductilities

Specimen	d_y^- [mm]	d_u^- [mm]	d_y^+ [mm]	d_u^+ [mm]	μ [-]	Dissipated Energy [kN.m]
REF	-7.17	-19.98	4.95	15.01	2.88	7.72
MF-EBRi	-7.19	-15.01	5.02	10	2.04 (-29%)	7.66 (-1%)
MF-EBRib	-6.55	-15.01	6.95	19.98	2.59 (-10%)	8.05 (4%)
MF-EBRd	-6.98	-15.01	4.35	10.02	2.21 (-23%)	11.01 (43%)
MF-FRPd	-6.69	-14.99	6.85	10.02	1.85 (-36%)	10.33 (34%)
NSMd	-7.15	-10.05	5.54	9.99	1.58 (-45%)	10.42 (35%)
NSMi	-14.04	-40.00	12.48	29.99	2.64 (-8%)	15.50 (101%)

Note: values in brackets represent the decrement in ductility when compared to the maximum ductility registered between both reference specimens.

4. CONCLUSIONS

From this work the major conclusions that can be pointed out are: all the strengthening strategies actually improved the load carrying capacity; the highest increase was achieved by solution NSMi (75%); the confinement provided by solution MF-EBRib compared to solution MF-EBRi added a marginal extra load carrying capacity; MF-FRPd performed better than MF-EBRd, which wasn't expected; all the strengthened specimens presented lower displacement ductility than REF one; the dissipated energy in the NSMi was extremely high when compared to all other specimens.

ACKNOWLEDGEMENT

This work is supported by FEDER funds through the Operational Programme for Competitiveness Factors – COMPETE and National Funds through FCT – Portuguese Foundation for Science and Technology under the project PTDC/ECM/74337/2006. The authors acknowledge the materials generously supplied by Hilti Portugal - Produtos e Serviços Lda. and S&P Clever Reinforcement Ibérica Lda.

REFERENCES

- Bank LC. (2004). Mechanically Fastened FRP (MF-FRP) Strips for Strengthening RC Structures – A Viable Alternative. *In: Proc. of 2nd International Conference on FRP Composites in Civil Engineering: CICE*, Adelaide, Australia, December 8-10, 2004, 12 pp.
- CEN (2004). EN 1998-1:2004 (E) Eurocode 8: Design of structures for earthquake resistance - Part 1: General rules, seismic actions and rules for buildings.
- Coelho, M., Fernandes, P., Sena-Cruz, J., Barros, J. (2011). Reforço sísmico de nós de pórtico em betão armado com laminados multidirecionais de CFRP. *Report no. 11-DEC/E-32*, University of Minho, Civil Engineering Department, 74 pp.
- Engindeniz, M., Kahn, L.F., Zureick, A. (2004). Repair and Strengthening of Non-Seismically Designed RC Beam-Column Joints: State-of-the-Art. *Research Report No. 04-4*. Georgia Institute of Technology, School of Civil and Environmental Engineering, Structural Engineering, Mechanics and Materials. 59 pp.
- NP EN 12390-3. (2009). Testing hardened concrete. Part 3: Compressive strength of test specimens.
- LNEC E397-1993. (1993). Concrete – Determination of the elasticity young modulus under compression. Portuguese specification from LNEC.
- NP EN 1992-1-1. (2010). Eurocode 2: Design of concrete structures – Part 1-1: General rules and rules for buildings.
- EN 10 002-1. (1990). Metallic materials - Tensile testing. Part 1: Method of test (at ambient temperature). CEN, Brussels, Belgium, 35 pp.
- Sena-Cruz, JM. (2004). Strengthening of concrete structures with near-surface mounted CFRP laminate strips. *PhD thesis*, Civil Engineering Department, University of Minho, Portugal, 216 pp.
- Sena Cruz, J.M., Barros, J.A.O., Coelho, M.R. (2010). Bond between concrete and multi-directional CFRP laminates. *Advanced Materials Research*, Vol. 133-134, 917-922.
- Sena Cruz, J.M., Barros, J.A.O., Coelho, M.R., Silva, L. (2011). Efficiency of different techniques in flexural strengthening of RC beams under monotonic and fatigue loading. *Construction & Building Materials*, 29:175–182.
- ISO 527-5. (1997). Plastics – Determination of tensile properties – Part 5: Test conditions for unidirectional fibre-reinforced plastic composites. *International Organization for Standardization*, Switzerland, 9 pp.